SOIL EROSION SUSCEPTIBILITY MAPPING OF IMO RIVER BASIN USING MODIFIED GEOMORPHOMETRIC PRIORITISATION METHOD

Peter C. Nwilo ⓘ , Caleb O. Ogbeta ⓘ , Olagoke E. Daramola ⓘ ,
Chukwuma J. Okolie ⓘ , Michael J. Orji ⓘ

Department of Surveying and Geoinformatics, University of Lagos, Lagos, Nigeria

Abstract: Gullies and other forms of erosion have been the greatest environmental problem and catastrophe in most high- and low-income countries. The challenge posed by soil erosion has compromised agricultural productivity, environmental biodiversity and food safety for the world's population. It is important to identify vulnerable areas to soil erosion in each region to initiate remedial measures. This study demonstrates the use of watershed morphometry coupled with weighted sum analysis (WSA) to estimate the soil erosion susceptibility of the Imo River Basin sub-watersheds (SWs) in South-Eastern Nigeria using satellite remote-sensing data and geographic information system (GIS) analysis. To this end, Shuttle Radar Topography Mission (SRTM), a Digital Elevation Model (DEM) with 30 m spatial resolution was used to extract and analyse 18 morphometric parameters including basic, linear, shape and relief. The method of receiver operating characteristics (ROC) curves was used to validate the model's prediction accuracy. This morphometry-based analysis resulted in the SWs being classified into zones of low, medium, high and very high erosion susceptibility. With regard to erosion susceptibility, 41.51% of the basin (2494.68 km²) is in the very high priority zone; while 10.50%, 44.33% and 3.66% of the basin are in the high, medium and low priority zones respectively. Validation of the final erosion susceptibility map showed a prediction accuracy of 81%. The use of satellite imagery and morphometric analysis in this study was cost- and time-effective for identifying areas susceptible to soil erosion.

Keywords: morphometry, weighted sum analysis, soil erosion susceptibility, SRTM, remote sensing, GIS, Imo River Basin

Corresponding author: Caleb O. Ogbeta, ogbetac@gmail.com

Introduction

Soil is a limited resource that is important for food production, carbon sequestration, water and nutrient management, contaminant filtration, biodiversity improvement, strong heritage, and climate regulation (Arshad, Martin 2002, Panagos et al. 2019). Due to population growth, economic progress and climate change, global soils are continually degrading (Montanarella et al. 2016). Soil erosion is a major cause of soil degradation as some forms of soil erosion by water (e.g. rill and gully) affect over 1 billion hectares globally (Lal 2003, Panagos et al. 2019). Anthropogenic activities as well as the resulting land-use changes (vegetation loss and growth in cropland) were the key reasons for a 2.5% rise in soil erosion by water between 2001 and 2012 (Borrelli et al. 2017).

The impacts of soil erosion go further than marginal land degradation. It has contributed to increased contamination and sedimentation in streams and rivers, blocking up these waterways and causing losses in the population of fish and other aquatic animals. Soil erosion impacts agricultural productivity, drinking water resource quality, soil and aquatic ecosystem health, and landscape aesthetic value (Fayas et al. 2019). The effect of water-driven soil erosion on the global market and food supply reflects an estimated financial loss of USD 8–40 billion, a decrease in food production of 33.7 million tonnes and a 48 billion cubic metres rise in water usage (Sartori et al. 2019). In nations such as Brazil, China, India and low-income households worldwide, these impacts are felt more intensely (Nkonya et al. 2016, Sartori et al. 2019). Cumulative expenditure projections to minimize the on-site impacts of land degradation (e.g. production losses) and its off-site implications (e.g. biodiversity losses and water body siltation) contribute to values of USD 400 billion per annum (Nkonya et al. 2016). However, these numerical values were obtained in soil loss studies utilising Universal Soil Loss Equation (USLE) or related techniques, without any consideration of gully erosion (Alencar et al. 2020).

With a view to sustainable development and environmental conversation, soil erosion by water has been highlighted as a vital issue to be confronted in the 21st century (Borrelli et al. 2017, Poesen 2018, Alencar et al. 2020). A global model by Borrelli et al. (2020) predicts that by the year 2070, soil erosion will massively increase from 30% to 66%, relative to the year 2015 estimates. The study also predicts that over 28 billion additional metric tons of soil will be lost annually if farming methods are not adjusted and steps are not taken to prevent climate change. This is about two-thirds >43 billion tons estimated for the year 2015. Tropical and sub-tropical countries with low to medium incomes are most vulnerable to a dramatic rise in erosion (Borrelli et al. 2020). In many parts of the world, extensive gully erosion caused by poor land management practices has had significant environmental effects. The contribution of gully erosion to the total soil loss from water erosion ranges from 10% to 94% worldwide, and in agricultural watersheds, it can account for up to 80% of the total soil erosion

(Capra, Scicolone 2002, Poesen et al. 2003, Gao et al. 2013). According to Nigeria Erosion and Watershed Management Program (NEWMAP) (2012), southern Nigeria is affected by massive gully erosion and there are an estimated 3000 gullies in rural or urban landscapes within the region. It is therefore critical for researchers and policymakers of these countries to explore erosion extent, identify possible hotspots, and work with stakeholders to soften the impact.

Poesen et al. (2003) identified gully erosion as a process that characterises runoff water which accumulates and often reoccurs in narrow channels and, over short periods thereby removing the soil from the narrow region to sizeable depths. Bernard et al. (2010) described the process of gully erosion as a mechanism that primarily starts during extreme rainfall events by eroding one channel or a series of channels due to the intensity of surface water discharge. Gullies contribute to land loss and desertification, as well as growing threats to the environment and society. Since the early 20th century, soil degradation has been a concern and according to estimates by the United States Department of Agriculture (USDA) and the National Conservation Congress, over 44,000 km² of global land has been abandoned due to extreme erosion (Alencar et al. 2020). This number had risen to over 200,000 km² by the end of the 1930s (Alencar et al. 2020).

Among soil erosion mechanisms, gully erosion has a significant contribution to watershed sedimentological processes, as it is also the primary cause of sediment displacement (Vanmaercke et al. 2016). Gullies also influence catchment connectivity (Verstraeten et al. 2006), enabling more sediments to enter water-bodies and therefore increasing siltation (De Arajuo et al. 2006). As they are extremely important in respect to erosion processes, gullies impose huge pressures on landscape development altering flood levels, increasing runoff and altering sediment dynamics (Valentin et al. 2005, Poesen 2018, Yibeltal et al. 2019). Gullies are also a major threat to humanity and its environment due to their effect on agricultural production, water availability, flooding, rubble flow and avalanches (Liu et al. 2016, Wei et al. 2018). Moreover, gullies do have a significant effect on the economy due to high costs of mitigation, reduced arable land, decreased freshwater reserves, improved connectivity of water

and sediment, and severe salinity of reservoirs. (Verstraeten et al. 2006, Pinheiro et al. 2016). The evaluation of the effects of gullies on production costs in an arid area of Israel showed that the expense of mitigating gullies accounted for over 5% of total investments and that production losses were as high as 37% (Valentin et al. 2005).

The mapping of erosion hazards is an important step for erosion control. A literature survey shows evidence of previous studies in this regard. For example, Nwilo et al. (2011) utilised Geographic Information Systems (GIS) as a method for identifying and mapping gully erosion hazards in Abia State, south-eastern Nigeria. A total of 171 gully erosion sites were coordinated using Global Positioning System (GPS) receivers, and a further 35 gully erosion sites were identified from a processed Digital Elevation Model (DEM). Relatedly, Okereke and Onu (2012) used remote sensing techniques to map the incidence of gully erosion in Okigwe, South-East Nigeria. In another study, Anejionu et al. (2013) adopted the Revised Universal Soil Loss Equation (RUSLE) to conduct a long-term evaluation of erosion hotspots in Southeast Nigeria. The study classified the zone into five erosion risk groups, ranging from very high to very low and included a spatial distribution mapping of erosion blackspots in the study area. By using the Revised USLE model, Chuenchum et al. (2020) analysed the evolving patterns of soil erosion and sediment yield from the effects of climate and land-use changes in the Lancang-Mekong River Basin, Southeast Asia. In most areas of the lower Mekong River Basin, the evolving environment and land use scenarios showed greater soil erosion and sediment yield. The results from this study could likewise serve as a knowledge resource in addressing the erosion issues in that region and in mitigating the possible effects. Applying the updated USLE formula in a GIS graphical user interface, a comprehensive assessment of soil erosion in the Kelani River Basin, Sri Lanka, effectively provided a range of spatially separate management strategies to deter erosion in the basin (Fayas et al. 2019). The study classified the Kelani River basin into five erosion risk groups: low, moderate, high, very high and extremely high. In addition to the categorisation, it included thematic maps on RUSLE parameters with applications in targeted conservation measures. Other

researchers have employed ground surveys for mapping erosion sites (Ofomata 1965, Ogbukagu 1976, Egboka, Okpoko 1984, Okagbue, Uma 1987, Akpokodje et al. 2010, Ezezika, Adetona 2011, Obiadi et al. 2011). However, the cumbersome nature of ground surveys including the high cost makes it a non-attractive option and not suitable for mapping extensive regions.

Morphometric mapping of drainage basins has been applied effectively over the last decade to classify sub-basins at various scales. It has found wide applications in the development, administration and prioritisation of sub-basins for soil and water management. Morphometry is the product of basic measurements and numerical modelling of soil surface setup, shape, and landform aspects (Adinarayana et al. 1995, Srivastava 2003, Jang et al. 2013). It is an essential element of hydrological and hydro-geological analysis (Agarwal 1998). It aids the understanding of hydrological characteristics, and its effects are useful inputs to a holistic approach for water resource conservation (Jawaharraj et al. 1998, Kumaraswami et al. 1998, Sreedevi et al. 2001). Morphometric analysis requires a calculation of the linear characteristics, channel network gradient, and contributing drainage basin ground slopes. It is an essential tool for prioritising sub-watersheds (SWs), without even considering the soil map (Biswas et al. 1999). Horton (1940) and Strahler (1950) conducted initial morphometric research in the field of hydrology. The movement of surface runoffs and sediments to a stream within the drainage basin is a basis for morphometric analysis (Chopra et al. 2005, Patel et al. 2013, Ameri et al. 2018). For example, Gajbhiye et al. (2014) used morphometric parameters to define critical sub-basins of the Manot river catchment of Madhya Pradesh in India, which were hurting from severe soil erosion. Ameri et al. (2018) also used morphometric parameters to prioritise the erodibility of 36 SWs of the Ghaemshahr Basin of Mazandaran Province in Iran. Rahaman et al. (2015) prioritised Kallar drainage basin SWs based on morphometric features, by using Fuzzy Analytic Hierarchy Process (AHP) and GIS.

It is evident that erosion poses a major challenge to the protection of soil and water supplies in South-Eastern Nigeria. Moreover, lasting results are yet to be attained by several government

intervention efforts such as the Nigeria Erosion and Watershed Management Program (NEWMAP) which was set up to curb the erosion threat in the region. A literature survey has not shown any evidence of the use of morphometric parameters in comprehensively modelling erosion processes and prioritising erosion-prone areas of catchment zones within South-Eastern Nigeria. Decision-makers in government, policy strategists, and soil and water conservationists require an understanding of the location and magnitude of erosion occurrence, now and in the future. This study aims to apply morphometric analysis for identifying areas susceptible to soil erosion within the Imo River Basin of South-Eastern Nigeria. Erodibility prioritisation of SWs was carried out through ranking and correlation analysis using the modified weighted sum analysis (WSA) approach. This study seeks to inform efforts aimed at mitigating the risk of erosion both locally and internationally by contributing to the knowledge base on erosion mapping and management. This caters to the vision of the United Nation's Sustainable Development Goals (SDGs) for life on land, and sustainable cities and communities.

Materials and methods

Study area

The Imo River Basin in South-Eastern Nigeria, West Africa has a total area of 2494.68 km². Geographically, it is located between latitudes 4°50′–6°00′N, and longitudes 7°05′–7°35′E. The Imo River originating from Okigwe in Imo State is the major river draining the basin (Amangabara 2015). The maximum elevation is found in the upper part of the basin with a height of 417 m above mean sea level (MSL), and the minimum height is in the lower part of the basin with a height of 5 m above MSL. The basin extent is shared by three dominant states namely – Imo, Abia and Rivers. Figure 1 presents a map showing the location of the Imo River Basin. The surrounding states have a hot, semi-hot equatorial type of climate. The area experiences heavy rainfall, with a mean annual precipitation of 2000–2400 mm and an average number of 152 rainy days especially during the wet season (April–October). The distribution

of superficial precipitation is skewed, with highs in July and September and a 2-week break in August. The rainy season starts in March and lasts until October or early November (NIMET 2019). Rainfall also hits its highest at night and during the early morning hours. The greater annual levels of rainfall and days of rainfall contribute to significant amounts of runoff. Differences in the amount of rainfall happen from year to year, however, usually between 1990 and 2200 mm (NIMET 2019). As a result, agricultural practices require little irrigation. This also promotes luxuriant forests beyond agriculture and recharging water sources from the soil and surface. Relative humidity during the dry and rainy seasons alternates between 75 and 90%. January to March are the hottest months, with annual average temperatures >20 °C.

The Imo River Basin is predominantly occupied by the Igbo-speaking tribe. With good soil for agriculture and water for fishing, the main occupation is farming and fishing as it provides a source of livelihood to the populace. Extraction of minerals such as crude oil by both skilled and unskilled labourers are also important activities within the basin. Manufacturing industries abound in this region's metropolitan areas. The whole South-East zone falls within Nigeria's forest and derived savanna belt. Much of the forestland has been transformed into oil palm tree-dominated farmlands and palm bushes. The region's major environmental concerns are deforestation, soil erosion and biodiversity depletion (Okali et al. 2001).

Data acquisition

This study utilised the Shuttle Radar Topography Mission (SRTM) v3.0 Global DEM acquired from the United States Geological Survey (USGS) web portal (earthexplorer.usgs. gov/). The SRTM DEM is provided in 1 × 1 tiles at 1 arc-second (30 m) and is defined on WGS 84 datum. It is also referenced to the EGM96 geoid model. Hence its heights are orthometric with vertical units in metres. The SRTM DEM's global coverage provides tremendous advantages for wide-area environmental modelling, especially when data availability is a problem. SRTM v3.0 which was released in September 2014 reveals the total detail of the world's landforms as originally
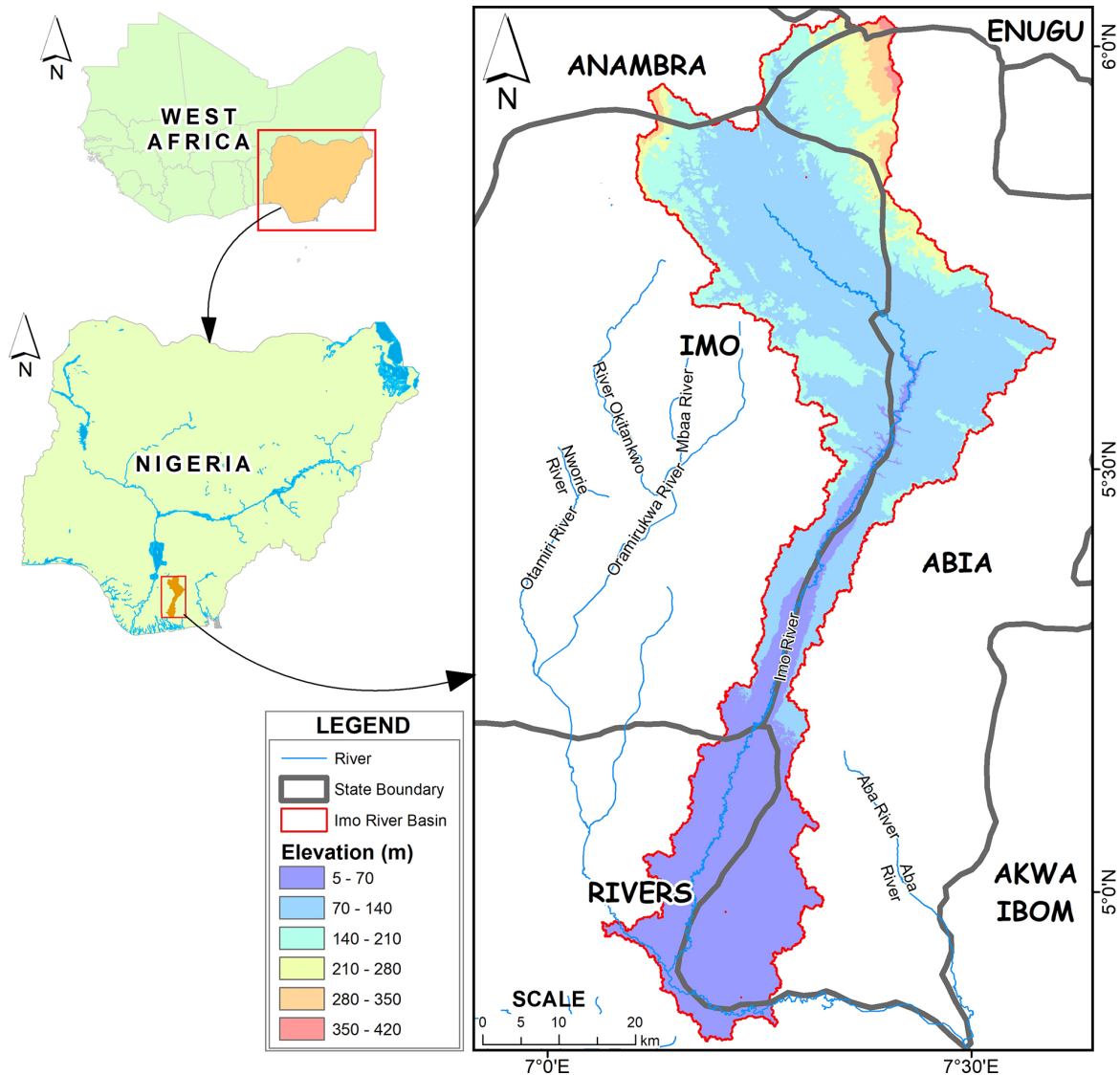
Fig. 1. Map showing the location of the study area.

captured by SRTM in the year 2000 (NASA JPL 2014). However, in providing reasonably reliable data to define drainage basin morphometry, several studies have shown that SRTM DEM is far better than the Advanced Spaceborne Thermal Emission and Reflection Radiometer (ASTER) DEM (Sun et al. 2003, Farr et al. 2007, Forkuor, Maathuis 2012, Patel et al. 2016). Figure 2 presents a workflow of the methodology.

DEM pre-processing and watershed mapping

DEM pre-processing is the first stage of the processing carried out on the DEM to make it more hydrologically correct and to improve on its terrain characterisation. The pre-processing
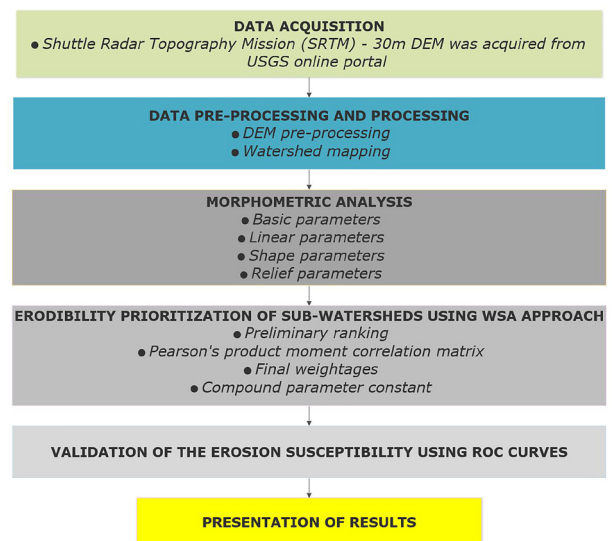

Fig. 2: Methodology workflow.

steps to be implemented are dependent on the type of terrain, and on the type of analysis to be carried out. The following pre-processing steps were executed within the ArcGIS 10.3 software environment – fill sinks, flow direction and flow accumulation. Thereafter, the watershed was delineated. The delineated watershed boundary was further segmented into SWs using the ArcHydro extension tools for ArcGIS 10.3. The drainage network of the SWs was extracted from the pre-processed DEM using the ArcHydro tools. ArcHydro uses a rational, efficient and reliable algorithm. In the next phase, the stream ranking (stream ordering) was carried out following the stream ranking system initially introduced by Horton (1945) and later amended by Strahler (1964). According to Strahler (1964), all rivers and streams of the fingertips are designated as streams of the first order and where two of them join; they form a stream of second order. Similarly, two streams of the second order join to form a stream of the third order, and so forth. Stream order increases only when streams of the same order converge. The convergence of a first-order and second-order link will therefore remain a second-order link, instead of creating a third-order link. The categorisation of rivers and streams within drainage basins can be accomplished by conventional methods such as using topographic maps and ground observations, or by using advanced techniques such as remote sensing and GIS (Macka 2001, Maidment 2002, Altaf et al. 2014).

Morphometric analysis

The morphometric analysis includes linear character estimation, channel network slope and contributing drainage basin ground slopes (Nautiyal 1994). The morphometric analysis for the different sub-basins was carried out by measuring the linear, shape and relief morphometric parameters of the basin. Areas and perimeters of the SWs were assessed by measuring the geometry of the derived sub-watershed polygons in the ArcGIS environment. Morphometric analysis is based on the overall drainage system activity. The drainage pattern refers to the spatial correlation between streams or rivers which may be impacted by the region's steepness, soil, rock rigidity, framework and geological history inequalities

in their erosion. The morphometric research uses some very important elements (linear, shape and relief parameters) to prioritise the SWs in water supply management. In this study, extraction and evaluation of the morphometric parameters in each of the SWs were ranked using their relationship to soil erodibility. The overall number of ranks assigned in this method is based upon the number of watersheds. Ranks were numbered from 1 to 25, based on the number of SWs delineated. Rank 1 was assigned in such a way that the parameter value represents the maximum contribution to erodibility and rank 25 is a minimum contribution. The formulas used to derive the necessary morphometric parameters pertaining to linear, areal, and relief aspects of the watershed are presented in Table 1.

Erodibility prioritisation of SWs using WSA approach

Erodibility prioritisation is the hierarchical ranking of various SWs in relation to soil erodibility, and the required soil and water conservation measures are taken according to the priority order. The WSA approach is effective and ideally suited to prioritizing watersheds. In the present study, sub-watershed wise delineation was done by using a newly developed prioritisation methodology where geospatial approaches are coupled with a statistical approach to allow the correct sub-watershed ranking, by avoiding the individual bias associated with several influencing parameters. Various morphometric parameters were rated in this method in terms of their relationship with erodibility, and correlation analysis among these parameters was performed. Therefore, it is hypothesised that an incentive exists to rectify the incorrect findings in order to increase the prioritisation accuracy. This method was useful in generating and assigning weights to each input variable according to their significance.

Secondly, the correlation between erosion assessment (morphometric) parameters using Pearson's product-moment correlation (r) was identified. The sum of all correlations in the columns was calculated and recognised as 'sum of correlation'. The totals of the 'sum of correlation' yielded the 'grand total'. Also, the final weights (Fw) of the morphometric parameters were

calculated by dividing the 'sum of the correlation coefficient' of each parameter by the grand total of correlations (Table 6).

The Fw were calculated using Eq. (1).

$$\text{Final weight (Fw}i) = \frac{\text{Sum of correlation coefficient}}{\text{Grand total of correlations}} \quad (1)$$

Finally, using Eq. (2), the compound parameter constant (Cpc) values of all SWs in the Imo-River Basin were calculated based on the weights of each morphometric parameter (metrics). A final erosion susceptibility map of the study area was prepared using the Cpc values.

$$\text{Cpc} = \sum(\text{Pr}i \times \text{Fw}i) \quad (2)$$

where:
- Pri is the preliminary rank of ith parameter for sub-watershed, and
- Fwi is the final weight of the same ith parameter.

Table 1. Formulas adapted for the computation of morphometric parameters.

S/N	Morphometric parameter	Formula	Unit	Reference
1	Basin area (A)	The area enclosed by the watershed (GIS software analysis)	km	Horton (1945)
2	Basin perimeter (P)	The perimeter of the watershed (GIS software analysis)	km	Horton (1945)
3	Basin length (Lb)	Distance from outlet to the farthest point on basin boundary (GIS software analysis)	km	Schumm (1956)
4	Stream order (U)	Hierarchical order	[–]	Strahler (1964)
5	Number of streams (Nu)	Total stream number of all orders (GIS software analysis)	[–]	Strahler (1964)
6	Total stream length (L)	Total stream length of all orders	km	Horton (1945)
7	Bifurcation ratio (Rb)	Rb = Nu / (Nu + 1) where Rb = Bifurcation ratio; Nu = Total no. of stream segments of order 'u'; Nu + 1 = Number of segments of the next higher order.	[–]	Schumm (1956)
8	Mean bifurcation ratio (Rbm)	Rbm = Average of bifurcation ratios of all orders	[–]	Strahler (1957)
9	Drainage density (Dd)	D = Lu / A where D = Drainage density; Lu = Total stream length of all orders; A = Basin area (km²)	km km^{-2}	Horton (1945)
10	Stream frequency (Fs)	Fs = Nu / A where Fs = Stream frequency; Nu = Total no. of streams of all orders; A = Basin area (km²)	no km^{-2}	Horton (1945)
11	Drainage texture (Dt)	Dt = Nu / P where Dt = Drainage texture; Nu = Total no. of streams of all orders; P = Basin Perimeter (km)	no km^{-1}	Horton (1945)
12	Elongation ratio (Re)	Re = 2 / Lb sqrt (A / π) where Re = Elongation ratio; A = Basin area (km²); π = 'Pi' value i.e. 3.14; Lb = Basin length	[–]	Schumm (1956)
13	Circulatory ratio (Rc)	Rc = 4 × π × A / P² where Rc = Circularity ratio; π = 'Pi' value i.e. 3.14; A = Basin area (km²); P = Basin Perimeter (km)	[–]	Miller (1953)
14	Form factor (Rf)	Rf = A /Lb² where Rf = Form factor; A = Basin area (km²); Lb² = Square of basin length	[–]	Horton (1932)
15	Compactness coefficient (Cc)	Cc = P / 2 sqrt (πA) where Cc = Compactness Coefficient; P = Basin perimeter (km); A = Basin area (km²)	[–]	Horton (1945)
16	Basin Relief (H)	H = Maximum relief − Minimum relief	m	Horton (1945)
17	Relief ratio (Rh)	Rh = H / Lb where Rh = Relief ratio; H = Basin relief; Lb = Basin length	[–]	Schumm (1956)
18	Ruggedness number (Rn)	Rn = Dd × (H / 1000) where Rn = Ruggedness Number; Dd = Drainage density; H = Basin relief	[–]	Strahler (1968)

Validation of the erosion susceptibility

To systematically and qualitatively evaluate the erosion susceptibility metrics, the method of receiver operating characteristics (ROC) curves was used to evaluate the model's prediction accuracy. ROC curves are useful in evaluating the performance of binary classifiers (Zhang et al. 2015) and can discriminate between the observed and predicted variables based on the logistic regression S-shaped curve. This validation technique is also known as relative operating characteristics (Pontius, Schneider 2001). The ROC curve technique follows a binary classification rule which results in four potential outcomes: true positive, true negative, false positive, and false negative. If a correct outcome is properly identified as positive, a true positive exists, while a false positive defines a negative outcome as being incorrectly positive. On the negatives, if a negative outcome is properly recognised as negative, a true negative exists, and a false negative wrongly recognises a true result as negative (Carter et al. 2016). The relationship between the sensitivity and 1 – specificity is graphically represented as the ROC curve and the area under the curve (AUC) is the accuracy of the predicted results. Sensitivity is characterised as the measure of positives correctly identified as such or the likelihood of a positive test, often referred to as the true-positive rate Eq.

(3). Specificity is the proportion of negatives correctly classified as such or the possibility of a negative test. This is also referred to as the true-negative rate. The false positive rate (1 – specificity) is the proportion of incorrect positive results that are actually negative Eq. (4). The false negative rate (1 – sensitivity) is the proportion of incorrect results that are actually positive (Nelson et al. 2005). By plotting the true-positive rate (sensitivity) on the y-axis against the false-positive rate (1 – specificity) on the x-axis, ROC curves are formed.

$$\text{True positive rate} = \frac{\text{True positives}}{\text{True positives + false negatives}} \quad (3)$$

$$\text{False positive rate} = \frac{\text{True negatives}}{\text{True negatives + false positives}} \quad (4)$$

For the validation of the erosion susceptibility result, the locations of prevalent erosional occurrences (shown in Table 2) were obtained from the literature and records of recent events from online sources (Amangabara et al. 2015, Amangabara et al. 2018, Channels Television 2018). With this technique, the ROC curve tool embedded in the SPSS software environment was deployed and the ROC curve plot was produced where the AUC was determined. The coordinates of the curve are shown in Table 3.

Table 2. Descriptive information of the validation points.

Point no.	Location name	Erosion type	Easting [mE]	Northing [mN]	Average depth [m]	Area [km²]	Source(s)
1	Ideato North	Gully erosion	297084	650725	15–35	30.11–109.72	(Amangabara et al. 2015, Amangabara et al. 2018)
2	Ideato South		296988	643359	15–35	30.11–109.72	
3	Okigwe		317303	643221	–	0.68	
4	Obowo		319395	616106	05–20	8.39–30.12	Amangabara et al. (2015)
5	Ehime Mbano		309899	628529	–	0.55–2.09	
6	Umuahia North	Gully erosion	332166	617607	–	6.85–31.70	Channels Television (2018)
7	Aboh-Mbaise		309726	593501	–	0.76–1.53	
8	Unuimo	No active erosion	303363	636918	–	–	–
9	Ogwe		306703	551110	–	–	–
10	Obiaku		301950	540063	–	–	–
11	Nkpa		333293	623302	–	–	–
12	Ihitte-Uboma		316080	623687	–	–	–
13	Etche		293472	547770	–	–	–

Table 3. Coordinates of the ROC curve.

S/N	1	2	3	4	5	6	7	8	9	10	11	12
Sensitivity	1.000	1.000	1.000	1.000	0.833	0.667	0.500	0.333	0.333	0.333	0.167	0.000
1 – Specificity	1.000	0.714	0.429	0.286	0.286	0.286	0.286	0.286	0.143	0.000	0.000	0.000

Results and discussion

SWs analysis

The watershed processing resulted in the delineation of the Imo River Basin with 25 SWs. Figure 3 presents a map showing the basin's SWs, with SW5 (656.12 km²) being the largest sub-watershed and SW6 (35.53 km²) being the smallest sub-watershed in terms of areal extent. The Imo River which is the major river in the basin has its source in the Okigwe upland located in SW16, and flows north to south through SW15, SW14, SW10, SW8, SW7, SW5, SW3 downwards to the basin outlet (SW1). The river flows across some major towns such as Okigwe, Abekenta, Ugwuaku, Umuzi, Ezinachi, Ife, Okpuala and Abiama in each SW, having its longest length of flow (105 km) in SW5. It is joined at SW3 by its major tributary (Otamiri River) flowing from the north and exits the basin at SW1.

Analysis of basic parameters

The results of the computation of basic morphometric parameters are shown in Table 4. The drainage networks in the Imo River Basin transport water and sediments of the basin through a single outlet (Imo River), which is marked as the maximum order of the basin and conventionally the highest order stream (6th order) available in the basin considered as the order of the basin. Based on stream order, Imo River Basin was graded as 6th order with an area of 2494.68 km² and a perimeter of 746.72 km. Figure 4 presents a map showing the basin's stream order. The cumulative number of streams in the basin is 1954. The total length of the streams in various orders is 2746.06 km.

Some of the morphometric parameters are directly considered as soil erosion metrics and thus are referred to as erosion risk assessment parameters (Biswas et al. 1999). These include the

Table 4. Basic parameters of sub-watersheds (SWs) in the Imo River Basin.

| Sub-watershed ID	Basin area	Basin perimeter	Basin length	No. of streams	Total stream length	Elevation	
						Max	Min
	[km²]	[km]		[–]	[km]	[m]	
SW1	51.97	75.23	11.27	37	51.43	41	12
SW2	39.24	50.30	8.33	26	40.75	37	14
SW3	103.93	104.85	16.51	84	113.91	52	18
SW4	158.62	117.01	22.45	128	180.71	70	17
SW5	656.12	351.57	69.97	548	757.62	193	20
SW6	35.53	48.99	11.95	29	35.00	186	67
SW7	137.12	112.25	15.56	102	139.73	206	60
SW8	56.51	58.75	10.11	49	60.28	203	67
SW9	67.16	57.89	10.46	63	77.83	175	81
SW10	50.87	51.22	10.44	36	48.03	212	75
SW11	89.84	79.12	12.13	70	90.71	240	73
SW12	83.18	64.30	11.21	79	86.64	219	82
SW13	53.53	52.09	12.76	26	55.09	286	75
SW14	60.49	56.84	10.96	51	66.94	290	76
SW15	58.19	69.55	13.51	48	62.12	330	82
SW16	63.83	62.58	14.73	39	69.49	334	83
SW17	116.86	76.83	13.38	99	133.21	262	89
SW18	83.69	107.19	14.88	67	85.68	239	86
SW19	59.31	55.17	13.47	37	66.98	360	99
SW20	68.98	52.21	10.58	51	71.15	323	118
SW21	55.77	72.08	14.31	40	76.02	322	99
SW22	78.38	102.44	24.19	48	80.23	386	86
SW23	47.47	80.10	18.18	37	50.74	345	104
SW24	124.73	106.08	18.73	85	135.74	417	109
SW25	93.37	68.50	13.43	75	110.06	416	149
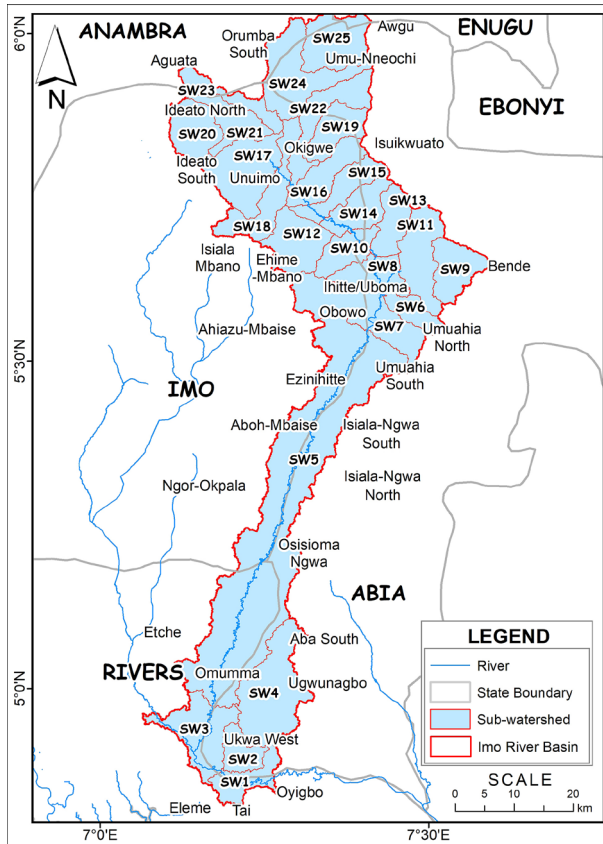
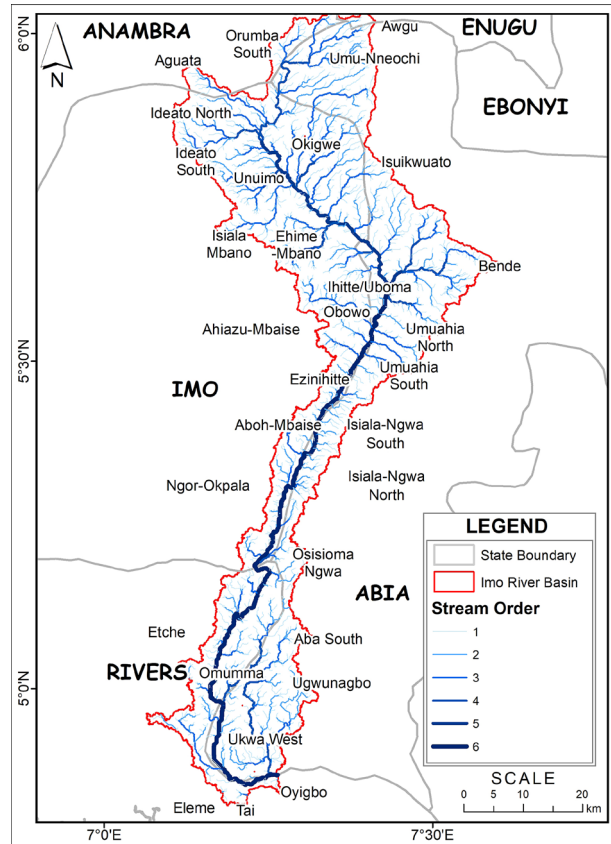Fig. 3. Sub-watershed map of Imo River Basin.

Fig. 4. Drainage map of Imo River Basin showing the stream order.

linear, shape and relief morphometric parameters as shown in Table 5. Linear and relief morphometric parameters have a direct/positive association with erodibility, i.e. the higher the values of these parameters, the greater the erodibility in the area and vice versa (Javed et al. 2009). In contrast, shape morphometric parameters have an inverse relation to erodibility i.e. the lower the values of these parameters, the higher the erodibility in the field of analysis and vice versa (Ratnam et al. 2005).

Analysis of linear morphometric parameters

These parameters include Drainage density (Dd), Stream frequency (Fs), Mean Bifurcation ratio (Rbm), and Drainage texture (Dt). A lower Dd in any watershed implies a porous sub-surface soil, strong vegetation-cover, low-relief and vice-versa (Harlin, Wijeyawickrema 1985, Nag, Chakraborty 2003, Prasad et al. 2008, Vaidya et al. 2013, Farhan, Anaba 2016, Farhan et al. 2017, Ali et al. 2018). A study by Asfaw and Workineh (2019) on Gumara and Ribb watershed, Ethiopia, shows a Dd of 0.26 km⁻¹ and 0.30 km⁻¹ which is

low and implies that the basin experience highly permeable sub-surface, low erosion exposure and better groundwater potential. Similarly, in the Imo River Basin, the lowest volume of Dd was observed in SW10 (0.94 km⁻¹), which indicates that this sub-watershed has a high degree of porosity among the other SWs, or it has the highest tendency to resist erosion if only the drainage parameter is taken as a metric for susceptibility to erosion.

The Fs has an inverse correlation with porosity and a positive correlation to watershed relief (Montgomery, Dietrich 1992). High Fs indicates that there is rocky terrain in the watershed and low infiltration ability which correlates to further erosion and vice versa (Altaf et al. 2014). In the Imo River Basin, the Fs ranges from 0.49 km⁻² for SW13 to 0.95 km⁻² for SW12. Based on the Fs, these results indicate that SW12 has the least infiltration capacity and hence, the highest susceptibility to erosion while SW13 has the least erosion susceptibility in terms of Fs only. The Rbm is a measure of the terrain's structural complexity and porosity and is thus negatively associated

Table 5. Linear, shape and relief parameters of sub-watersheds (SWs) in the Imo River Basin and its preliminary ranking with respect to soil erodibility.

Sub-watershed	Linear parameters				Shape parameters				Relief parameters		
	Dd	Fs	Rbm	Dt	Re	Rc	Rf	Cc	H	Rh	Rn
SW1	0.99 (23)	0.71 (18)	5.57 (2)	0.49 (23)	0.72 (14)	0.12 (5)	0.41 (14)	2.97 (21)	29 (24)	0.003 (22)	0.029 (24)
SW2	1.04 (16)	0.66 (21)	4.50 (7)	0.52 (21)	0.85 (19)	0.20 (14)	0.57 (19)	2.28 (12)	23 (25)	0.003 (21)	0.024 (25)
SW3	1.10 (9)	0.81 (9)	3.96 (17)	0.80 (13)	0.70 (13)	0.12 (6)	0.38 (13)	2.92 (20)	34 (23)	0.002 (25)	0.037 (23)
SW4	1.14 (6)	0.81 (10)	4.70 (6)	1.09 (5)	0.63 (7)	0.15 (10)	0.32 (7)	2.64 (16)	53 (22)	0.002 (24)	0.060 (22)
SW5	1.16 (4)	0.84 (6)	4.80 (4)	1.56 (1)	0.41 (2)	0.07 (1)	0.13 (2)	3.90 (25)	173 (12)	0.003 (23)	0.200 (12)
SW6	0.99 (24)	0.82 (8)	4.80 (5)	0.59 (19)	0.56 (4)	0.19 (13)	0.25 (4)	2.34 (13)	119 (20)	0.010 (18)	0.117 (20)
SW7	1.02 (21)	0.74 (15)	4.48 (8)	0.91 (8)	0.85 (20)	0.14 (8)	0.57 (20)	2.72 (18)	146 (16)	0.009 (19)	0.149 (16)
SW8	1.07 (14)	0.87 (3)	4.35 (12)	0.83 (11)	0.84 (18)	0.21 (16)	0.55 (18)	2.22 (10)	136 (19)	0.014 (11)	0.145 (17)
SW9	1.16 (3)	0.94 (2)	3.74 (21)	1.09 (6)	0.88 (22)	0.25 (23)	0.61 (22)	2.01 (3)	94 (21)	0.009 (20)	0.109 (21)
SW10	0.94 (25)	0.71 (19)	3.17 (24)	0.70 (14)	0.77 (15)	0.24 (18)	0.47 (15)	2.04 (8)	137 (17)	0.013 (13)	0.129 (19)
SW11	1.01 (22)	0.78 (14)	3.11 (25)	0.89 (10)	0.88 (21)	0.18 (12)	0.61 (21)	2.37 (14)	167 (14)	0.014 (10)	0.169 (14)
SW12	1.04 (15)	0.95 (1)	3.98 (16)	1.23 (3)	0.92 (25)	0.25 (24)	0.66 (25)	2.00 (2)	137 (18)	0.012 (16)	0.143 (18)
SW13	1.03 (18)	0.49 (25)	3.50 (22)	0.50 (22)	0.65 (10)	0.25 (20)	0.33 (10)	2.02 (6)	211 (10)	0.017 (7)	0.217 (10)
SW14	1.11 (8)	0.84 (5)	4.47 (9)	0.90 (9)	0.80 (16)	0.24 (17)	0.50 (16)	2.08 (9)	214 (9)	0.020 (2)	0.237 (9)
SW15	1.07 (13)	0.82 (7)	4.31 (13)	0.69 (15)	0.64 (8)	0.15 (11)	0.32 (8)	2.59 (15)	248 (6)	0.018 (5)	0.265 (7)
SW16	1.09 (10)	0.61 (24)	4.45 (11)	0.62 (18)	0.61 (6)	0.21 (15)	0.29 (6)	2.22 (11)	251 (5)	0.017 (6)	0.273 (6)
SW17	1.14 (5)	0.85 (4)	3.45 (23)	1.29 (2)	0.91 (24)	0.25 (21)	0.65 (24)	2.02 (5)	173 (13)	0.013 (14)	0.197 (13)
SW18	1.02 (19)	0.80 (12)	5.20 (3)	0.63 (17)	0.70 (12)	0.09 (2)	0.38 (12)	3.33 (24)	153 (15)	0.010 (17)	0.157 (15)
SW19	1.13 (7)	0.62 (22)	3.75 (19)	0.67 (16)	0.65 (9)	0.25 (19)	0.33 (9)	2.04 (7)	261 (4)	0.019 (4)	0.295 (5)
SW20	1.03 (17)	0.74 (16)	4.47 (10)	0.98 (7)	0.89 (23)	0.32 (25)	0.62 (23)	1.79 (1)	205 (11)	0.019 (3)	0.211 (11)
SW21	1.36 (1)	0.72 (17)	4.14 (14)	0.56 (20)	0.589 (5)	0.14 (7)	0.27 (5)	2.74 (19)	223 (8)	0.016 (9)	0.304 (4)
SW22	1.02 (20)	0.61 (23)	6.44 (1)	0.47 (24)	0.41 (1)	0.09 (4)	0.13 (1)	3.29 (22)	300 (2)	0.012 (15)	0.307 (3)
SW23	1.07 (12)	0.78 (13)	3.75 (20)	0.46 (25)	0.43 (3)	0.09 (3)	0.14 (3)	3.30 (23)	241 (7)	0.013 (12)	0.258 (8)
SW24	1.09 (11)	0.68 (20)	4.03 (15)	0.80 (12)	0.67 (11)	0.14 (9)	0.36 (11)	2.70 (17)	308 (1)	0.016 (8)	0.335 (1)
SW25	1.18 (2)	0.80 (11)	3.91 (18)	1.10 (4)	0.81 (17)	0.25 (22)	0.52 (17)	2.01 (4)	267 (3)	0.020 (1)	0.315 (2)

Preliminary ranks are shown in brackets.
Dd – drainage density; Fs – stream frequency; Rbm – mean bifurcation ratio; Dt – drainage texture; Cc – compactness coefficient; Re – elongation ratio; Rc – circulatory ratio; Rf – form factor; H – total basin relief; Rh – relief ratio; Rn – ruggedness number.

with the watershed's porosity. High Rbm suggests early hydrographic optimum with capacity for flood events during heavy rains leading to the deterioration of the soil surface (Howard 1990). Rbm's connection to an area's susceptibility to erosion is the same as that conveyed by Dd and Fs. Hence in this instance, the classification was the same as in the case of Dd and Fs. In the Imo River Basin, the Rbm ranges from 3.11 for SW11 to 6.44 for SW22. SW22 has the highest susceptibility to erosion in the study area according to Rbm results. The final linear morphometric parameter is the Drainage texture (Dt) that is strongly affected by the infiltration ability (Horton 1945). Low-infiltration regions will produce higher Dt and thus result in more erosion. The sub-watershed with the highest value of Dt in the Imo River Basin is SW5 (1.56 km⁻¹),

indicating that it is the most susceptible to erosion due to a low infiltration rate. The sub-watershed with the lowest Dt is SW23 (0.46 km⁻¹), and this suggests that it is less vulnerable to erosion based on the study of the drainage texture.

Analysis of shape morphometric parameters

The basin shape mainly regulates the rate at which the water is delivered to the secondary channel. These parameters include Elongation ratio (Re), Circulatory ratio (Rc), Form factor (Rf) and Compactness coefficient (Cc). In general, the Re ranges from 0.6 to 1.0 and is correlated with climate and geology (Schumm 1956, Strahler 1964). Re values close to 1.0 are transmitted to very low relief areas, while those values of 0.6–0.8 are correlated with high relief and steep

slopes on the ground (Dar et al. 2013). The study found that SW12 with the highest Re (0.92) was the least susceptible to erosion and, in comparison, SW22 with the lowest Re (0.41) was the most susceptible to erosion. The Rc is influenced primarily by characteristics such as stream length and frequency, geological structures, climate, relief, and gradient of the basin (Miller 1953). Rc values range from 0 (in line) to 1 (in one circle). In a related study of the SWs of the Shivganga River Basin India by Kadam et al. (2019), a low Rc (i.e. 0.19) indicated rapid discharge from the sub-watershed and consequently, a higher susceptibility to erosion (Kadam et al. 2019). Higher values reflect more basin-shaped circularity and vice-versa. The sub-watershed SW5 in the Imo River Basin with the lowest amount of Rc (0.07) indicates the highest vulnerability to erosion with Rc as the only criterion.

In this way, the Rf has an inverse correlation to erosion; the lowest Rf values are most susceptible to erosion. The Rf values are within the range of 0.1–0.8 (Horton 1932). High-shaped basins have high peak flows of shorter length whereas elongated drainage basins with low-shaped influences have lower peak flows of longer duration (Singh, Singh 2011, Farhan, Anaba 2016, Asfaw, Workineh. 2019). The results of the Rf derived from the SWs of the Imo River Basin differ from the minimum (0.13) for SW22 up to the maximum (0.66) for SW12. Thus, the Rf analysis places SW22 as being most susceptible to erosion. A watershed's Cc is directly related to the potential for watershed penetration. Therefore, the rating adopted was identical to that adopted by Rf. The lowest Cc was recorded for SW20 with a value of 1.79, which means that it has the minimum absorption potential and thus the highest erosion sensitivity. The highest was noticed in SW5 with a value of 3.90 implying that it has the highest capacity for infiltration.

Analysis of relief morphometric parameters

These parameters include Total Basin relief (H), Relief ratio (Rh), and Ruggedness number (Rn). The Total Basin relief (H) is the difference in altitude of the highest and lowest point of a basin valley floor. A strong correlation exists between the hydrological characteristics and a drainage basin's H (Schumm 1956). The H is an indicator of a drainage basin's total slope, as well as the ferocity of the erosion processes functioning on the basin slopes. In this case, the ranking system implemented was equivalent to the one implemented in the case of D, Fs and Rbm, since they all infuse the same erosive traits in any landscape. The lowest basin relief (i.e. 0.57) in a study conducted by Altaf et al. (2014) on the Rembiara Watershed, India was identified in one of the SWs, indicating its low steepness and hence low susceptibility to erosion. Similarly, the lowest value of H in the Imo River Basin was observed in SW2 (23 m) which demonstrated its low slope and therefore low risk to erosion. H's highest value was identified in SW24 (308 m), which is due to its high steepness and therefore higher sensitivity to erosion. The next parameter is the Rh that is specifically linked to the slope of the streams and the surface of the earth; which influences the hydrological processes and the watershed's erosion. The Rh basin has a direct correlation with the watershed's erodibility. In the Imo River Basin, the largest rate of Rh was in SW25 (0.020) and its lowest is for SW3 (0.002). Based on this analysis, SW25 is the most vulnerable to erosion compared with other SWs. The final parameter, Rn, is used to compute stream flood potential (Patton, Baker 1976). It symbolises the geometrical characteristics of the sub-basins of the Imo River Basin. Rn has a direct relationship with erodibility so that the erodibility also increases with increasing values of that parameter. The lowest value of Rn was observed for SW2 (0.024) which indicates that it has the lowest susceptibility to erosion. The highest value of Rn was obtained for SW24 (0.335) which means that it has the greatest susceptibility to erosion. In a study of the Dhidhessa River Basin in Ethiopia by Kabite and Gessesse (2018) the Rn of 3.1 indicated rough topography and susceptibility to soil erosion. Similarly, Kumar and Joshi (2016) derived an Rn value of 0.78 in another watershed and this was interpreted as having a steep slope and soil erosion susceptibility in the region.

Morphometry analysis-based erodibility prioritisation using WSA approach

After allocating ranks to the morphometric erosion potential parameters with respect to the relationship with erodibility, the correlation

matrix was constructed using Pearson's product-moment correlation (r). Several parameters are very highly correlated with each other, and this high level of interdependence is observed between parameters in similar categories (i.e. linear, shape or relief). However, there is a strong negative correlation (r = −0.96) between two shape parameters, the Cc and Rc, and also a strong positive correlation (r = 0.99) between two relief parameters, total basin relief (H) and Rn. The Fw of the parameters were calculated using the WSA approach (Table 6). The correlation matrix showed that the Rbm has a negative correlation with most of the morphometric parameters except the Cc which have a positive correlation (0.53). The Re has a strong positive correlation with Rc and Rf and a strong negative correlation

with Cc (−0.70). Also, Fs has the highest correlation with drainage texture (0.63).

In the WSA approach, the sum of correlation is the summation of the columns (Table 6) for Dd, Fs, Rbm, Dt, Re, Rc, Rf, Cc, H, Rh, Rn as:

$$\text{Sum of correlation for Rn} = [0.38 + (−0.29) + (−0.07) + (−0.07) + (−0.35) + 0.05 + (−0.34) + 0.00 + 0.99 + 0.80 + 1.00] = 2.10$$

Further, the grand total obtained from the sum of correlations (14.71) was used for calculating the final weight of each morphometric parameter using Eq. (1). This was used in the final prioritisation ranking. By assigning those weights to each parameter, a model was formulated to assess the priority. For example, the final weight of Rn is the

Table 6. Pearson correlation matrix of sub-watershed morphometric parameters.

Parameter	Dd	Fs	Rbm	Dt	Re	Rc	Rf	Cc	H	Rh	Rn
Dd	1.00	0.16 (0.44)	−0.14 (0.51)	0.28 (0.17)	−0.14 (0.52)	−0.05 (0.82)	−0.14 (0.51)	0.05 (0.80)	0.22 (0.29)	0.13 (0.55)	0.38 (0.06)
Fs	0.16 (0.44)	1.00	−0.11 (0.61)	0.63** (0.00)	0.35 (0.08)	0.04 (0.87)	0.39 (0.06)	−0.01 (0.98)	−0.33 (0.11)	−0.20 (0.34)	−0.29 (0.15)
Rbm	−0.14 (0.51)	−0.11 (0.61)	1.00	−0.22 (0.28)	−0.42* (0.04)	−0.51** (0.01)	−0.41* (0.04)	0.53** (0.01)	−0.04 (0.84)	−0.32 (0.12)	−0.07 (0.76)
Dt	0.28 (0.17)	0.63** (0.00)	−0.22 (0.28)	1.00	0.33 (0.11)	0.21 (0.31)	0.38 (0.06)	−0.08 (0.71)	−0.10 (0.63)	−0.13 (0.53)	−0.07 (0.75)
Re	−0.14 (0.52)	0.35 (0.08)	−0.42* (0.04)	0.33 (0.11)	1.00	0.67** (0.00)	0.99** (0.00)	−0.70** (0.00)	−0.35 (0.09)	0.11 (0.59)	−0.35 (0.09)
Rc	−0.05 (0.82)	0.04 (0.87)	−0.51** (0.01)	0.21 (0.31)	0.67** (0.00)	1.00	0.66** (0.00)	−0.96** (0.00)	0.06 (0.79)	0.52** (0.01)	0.05 (0.83)
Rf	−0.14 (0.51)	0.39 (0.06)	−0.41* (0.04)	0.38 (0.06)	0.99** (0.00)	0.66** (0.00)	1.00	−0.68** (0.00)	−0.33 (0.11)	0.10 (0.63)	−0.34 (0.10)
Cc	0.05 (0.80)	−0.01 (0.98)	0.53** (0.01)	−0.08 (0.71)	−0.70** (0.00)	−0.96** (0.00)	−0.68** (0.00)	1.00	−0.01 (0.98)	−0.51* (0.01)	0.00 (0.99)
H	0.22 (0.29)	−0.33 (0.11)	−0.04 (0.84)	−0.10 (0.63)	−0.35 (0.09)	0.06 (0.79)	−0.33 (0.11)	−0.01 (0.98)	1.00	0.81** (0.00)	0.99** (0.00)
Rh	0.13 (0.55)	−0.20 (0.34)	−0.32 (0.12)	−0.13 (0.53)	0.11 (0.59)	0.52** (0.01)	0.10 (0.63)	−0.51* (0.01)	0.81** (0.00)	1.00	0.80** (0.00)
Rn	0.38 (0.06)	−0.29 (0.15)	−0.07 (0.76)	−0.07 (0.75)	−0.35 (0.09)	0.05 (0.83)	−0.34 (0.10)	0.00 (0.99)	0.99** (0.00)	0.80** (0.00)	1.00
Sum of correlation	1.76	1.63	−0.71	2.22	1.50	1.69	1.63	−1.35	1.92	2.31	2.10
Grand total	14.71	14.71	14.71	14.71	14.71	14.71	14.71	14.71	14.71	14.71	14.71
Final weights	0.120	0.111	−0.048	0.151	0.102	0.115	0.111	−0.092	0.130	0.157	0.143

Significance (2-tailed) are shown in brackets.
** – correlation is significant at the 0.01 level (2-tailed).
* – correlation is significant at the 0.05 level (2-tailed).
Dd – drainage density; Fs – stream frequency; Rbm – mean bifurcation ratio; Dt – drainage texture; Cc – compactness coefficient; Re – elongation ratio; Rc – circulatory ratio; Rf – form factor; H – total basin relief; Rh – relief ratio; Rn – ruggedness number.

sum of correlation i.e. 2.10 divided by the grand total of 14.71 (Table 6). The resulting value (0.143), was used for the calculation of the Cpc, and further used in the SWs' prioritisation and final ranking.

Similarly, the Cpc for SW1 was calculated as follows:

Cpc for SW1 = (0.120 × 23) + (0.111 × 18) + (−0.048 × 2) + (0.151 × 23) + (0.102 × 14) + (0.115 × 5) + (0.111 × 14) + (−0.092 × 21) + (0.130 × 24) + (0.157 × 22) + (0.143 × 24) = 19.78

In addition, the Cpc values of the 25 SWs in the Imo River Basin were calculated using the WSA method, and prioritization ranking allocation was incorporated as presented in Table 7. The first priority (1) was given to sub-watershed 5 with a Cpc value of 6.25, with the second priority (2) being sub-watershed 21, with a Cpc value of 7.51. The Imo River Basin's SWs were further classified into four (4) priority groups based on natural breaks (Jenks method) of the Cpc values – very high priority (6.25–8.52) covering 1035.64 km² or 41.51%

of the basin area (2494.68 km²), high priority (8.52–10.50) covering 262.01 km² or 10.50% of the basin area, medium priority (10.50–17.56) covering 1105.82 km² or 44.33% of the basin area and low priority (17.56–21.77) covering 91.21 km² or 3.66% of the basin area. Of the 25 SWs in the Imo River Basin, 'SW5, SW21, SW25, SW24, SW15, and SW23' fall in very high priority; 'SW14, SW19, SW22, and SW16' fall in high priority; 'SW17, SW4, SW18, SW11, SW8, SW13, SW3, SW20, SW6, SW7, SW9, SW12 and SW10' fall in medium priority; whereas 'SW1 and SW2' fall in the low priority category. The highest priority suggests a greater degree of erosion exists in the sub-watershed and is a potential area for soil conservation measures to be implemented. Figure 5 shows the final erosion susceptibility map of the study area based on the Cpc values.

These results show an improved accuracy in prioritising sub-basins than other methods such as the multi-criteria evaluation approach (Altaf et al. 2014, Alvarado et al. 2016, Vollmer et al. 2016), compound factor analysis (Patel et al. 2012,

Table 7. Watershed prioritisation and final ranking for erosion susceptibility.

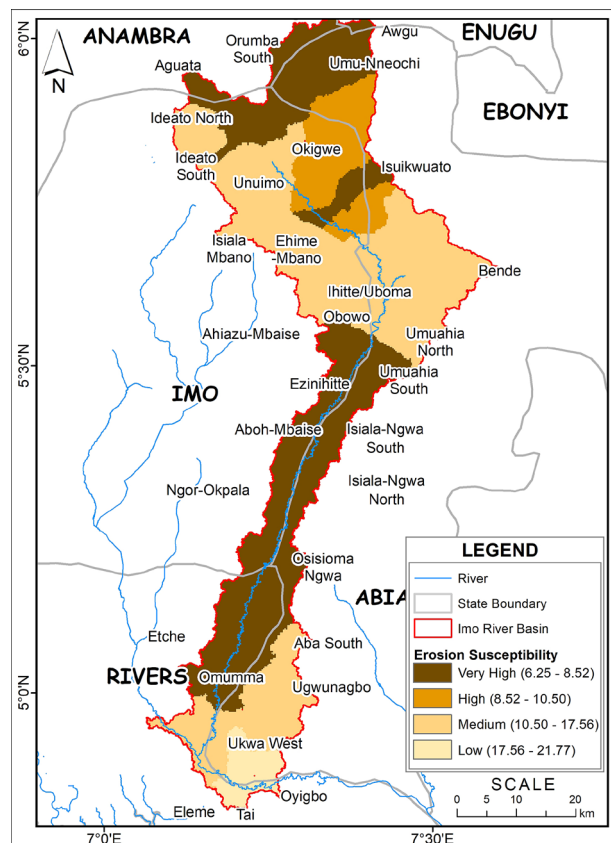| Sub-watershed ID	Compound parameter constant value	WSA final ranking
SW1	19.78	24
SW2	21.77	25
SW3	15.06	17
SW4	13.25	12
SW5	6.25	1
SW6	15.84	19
SW7	15.89	20
SW8	14.48	15
SW9	16.40	21
SW10	17.56	23
SW11	14.45	14
SW12	16.91	22
SW13	14.90	16
SW14	9.74	7
SW15	8.13	5
SW16	10.50	10
SW17	13.04	11
SW18	13.39	13
SW19	10.10	8
SW20	15.53	18
SW21	7.51	2
SW22	10.24	9
SW23	8.52	6
SW24	7.98	4
SW25	7.80	3

Fig. 5. Erosion susceptibility map of the study area based on Cpc value. Cpc, compound parameter constant.

Mohammed et al. 2018) and compound parameter technique (Hlaing et al. 2008, Rawat et al. 2014).

In the past, governmental intervention efforts were initiated in some of these communities to arrest the spate of erosion. For example, gully sites at Umueshi, Amanato and Ntueke in the very high susceptibility area were within the zones marked for rehabilitation by the Imo State Nigeria Erosion and Watershed Management Project (IMO-NEWMAP) in 2014. One of the objectives of IMO-NEWMAP was to reduce the longer-term erosion vulnerability of the communities. In recent media reports on gully erosion in South-East Nigeria, the Isiokpo, Okpulu and Obidioukwu communities of Ideato North Local Government Area (LGA) of Imo State within the very high erosion susceptibility area have received a lot of attention. Residents of these three communities fled their homes on the 1st of September 2018, amid significant gully erosion after heavy rainfall (Channels Television 2018). Chiemelu et al. (2013) also described the Okigwe upland, which falls within the highly susceptible region, as a trouble spot for gully erosion.
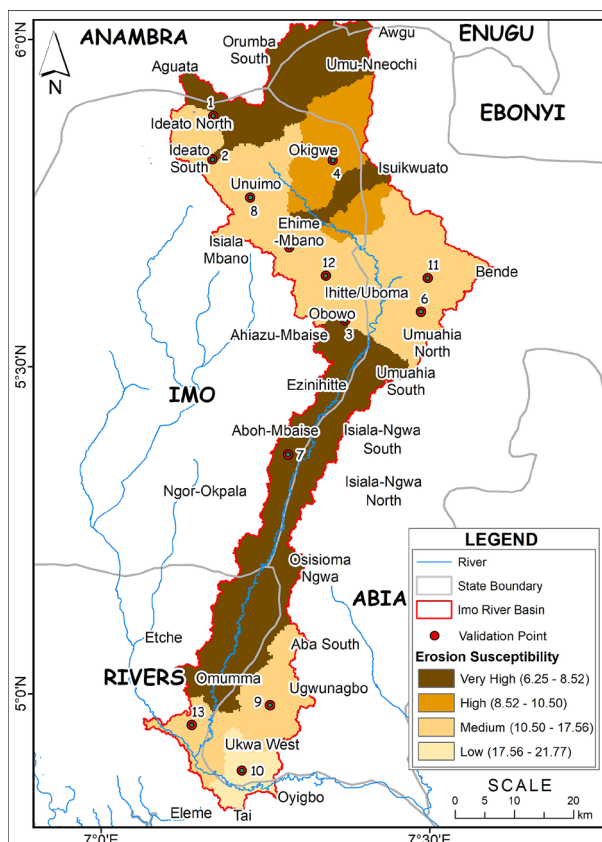
Fig. 6. Overlay of validation points on the erosion susceptibility map.

Model performance evaluation

The validation points are overlaid on the erosion susceptibility map in Figure 6. The ROC curve plot shown in Figure 7 has the false-positive rate on the X-axis and the true-positive rate on the Y-axis. The AUC value computed is 0.810 which implies a prediction accuracy of 81% of the morphometry-based model.
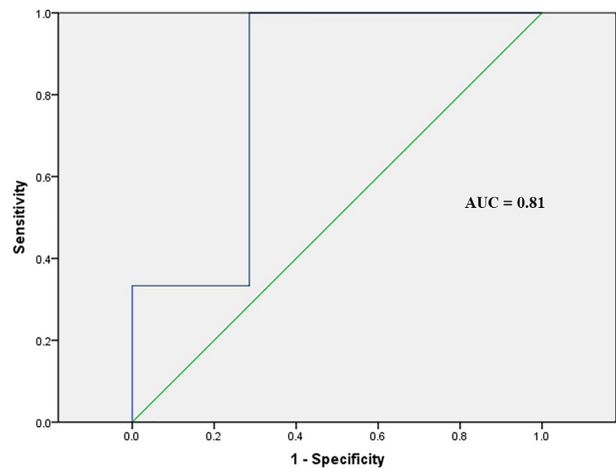

Fig. 7. The ROC technique validation result. ROC, receiver operating characteristics.

Conclusions

This study successfully classified the Imo River Basin in South-East Nigeria into priority zones based on susceptibility to soil erosion, using a modified geomorphometric prioritisation approach. Soil erosion is a serious environmental problem in the Imo River Basin. Identifying the susceptibility to erosion is a critical measure for ensuring adequate preparedness. This study presents a simple methodology and low-cost strategy for mapping erosion susceptibility on a sub-watershed basis within the Imo River Basin. Several parameters are very highly correlated with each other, and this high level of interdependence is observed between parameters in similar categories (i.e. linear, shape or relief). However, there is a strong negative correlation (r = −0.96) between two shape parameters, the Cc and Rc. Based on the analysis of linear, shape and relief morphometric parameters, this study has shown the varying levels of erosion susceptibility in the Imo River Basin. For example, in terms of the linear morphometric parameters, the lowest

volume of Dd which was observed in SW10 indicates a high degree of porosity and a high tendency to resist erosion. Similarly, the high Fs in SW12 which suggests a low soil infiltration puts it at a higher risk of erosion. In terms of the shape parameters, SW22 and SW 5 which had the lowest Re and lowest Rc were also deemed very susceptible to erosion. The minimum absorption potential of SW20 is related to its low Cc, and thus makes it highly susceptible to erosion. Analysis of the relief morphometric parameters showed that SW2 had the lowest total basin relief which implies a low-level relief and low susceptibility to erosion. The Rn which has a relationship with stream flood potential was also computed. SW2 had the lowest Rn thus indicating a low susceptibility to erosion.

The detection of vulnerable areas is a criterion for the design and execution of appropriate soil and water conservation management practices in the Imo River Basin. The results from this study show that 41.51% (1035.64 km^2) of the total area (2494.68 km^2) falls under the very-high priority group i.e. areas that are highly susceptible to erosion, 10.50% (262.01 km^2) falls under the high erosion susceptibility class, 44.33% (1105.82 km^2) in the medium susceptibility class and 3.66% (91.21 km^2) in the low erosion susceptibility class. The prediction accuracy of the erosion susceptibility result was determined as 81% using the ROC curve technique. These SWs need to be taken up immediately by decision-makers and soil and water managers to enforce conservation measures for preventing further erosion.

Soil erosion can be mitigated by adopting sustainable land management practices such as tree planting, zero or reduced tillage, stone bunds, enclosures, terracing and check dams. Also, policy incentives should be provided to encourage the adoption of these practices. This will lead to reduced soil loss and additional household incomes thereby improving livelihoods. Future research priorities should include: sub-surface flow erosion processes, prediction models, application of geographic data and assessment tools in soil erosion control, and issues regarding the adoption of conservation strategies by farmers and individuals. Further research directions include the evaluation of the disparities in the adaptive capacity and resilience of the inhabitants within the river basin to erosion and other ecological disasters. This current study demonstrates that morphometric analysis applied to satellite imagery is a timely and cost-effective approach for providing useful information that can help decision-makers develop more sustainable and environmentally friendly strategies for soil and water conservation.

Acknowledgements

Conflicts of interest

The authors declare that they have no conflicts of interest.

Funding

Authors' contribution

Peter C. Nwilo: project administration, resources, supervision. Caleb O. Ogbeta: conceptualisation, formal analysis, methodology, visualisation, writing – original draft preparation, reviewing and editing. Olagoke E. Daramola: conceptualisation, methodology, validation, visualisation, writing – reviewing and editing. Chukwuma J. Okolie: methodology, validation, visualisation, writing – reviewing and editing. Michael J. Orji: visualisation, writing – reviewing and editing.

References

Adinarayana J., Krishna R.N., Rao K., 1995. An integrated approach for prioritization of watersheds. *Journal of Environmental Management* 44: 375–384. DOI 10.1016/S0301-4797(95)90374-7.

Agarwal C.S., 1998. Study of drainage pattern through aerial data in Naugarh area of Varanasi district. *U.P. J of Indian Soc of Rem Sensing* 26: 169–175. DOI 10.1007/bf02990795.

Akpokodje E.G., Tse A.C., Ekeocha N., 2010. Gully erosion geohazards in Southeastern Nigeria and management implications. *Scientia Africana* 9(1): 20–36.

Alencar P.H.L., de Araújo J.C., dos Santos Teixeira A., 2020. Physically based model for gully simulation: Application

to the Brazilian semiarid region. *Hydrology and Earth System Sciences* 24(8): 4239–4255. DOI 10.5194/hess-24-4239-2020.

Ali U., Ali S.A., Ikbal J., Bashir M., Fadhi M., Ahmad M., Al Dharab H., Ali S., 2018. Soil erosion risk and flood behavior assessment of Sukhang catchment, Kashmir basin: Using GIS and remote sensing. *International Journal of Remote Sensing GIS* 7(1): 1–8. DOI 10.4172/2469-4134.1000230.

Altaf S., Meraj G., Romshoo S.A., 2014. Morphometry and land cover based multi-criteria analysis for assessing the soil erosion susceptibility of the western Himalayan watershed. *Environmental Monitoring and Assessment* 186(12): 8391–8412. DOI 10.1007/s10661-014-4012-2.

Alvarado A., Esteller M.V., Quentin E., Exposito J.L., 2016. Multi-criteria decision analysis and GIS approach for prioritization of drinking water utilities protection based on their vulnerability to contamination. *Water Resource Management* 30: 1549–1566. DOI 10.1007/s11269-016-1239-4.

Amangabara G.T., 2015. Drainage morphology of Imo basin in the Anambra–Imo river basin area, of Imo state, southern Nigeria. *Journal of Geography, Environment and Earth Science International* 3(1): 1–11. DOI 10.9734/jgeesi/2015/17114.

Amangabara G.T., Njoku J.D., Iwuji M.C. 2018. People's perception of soil erosion and its impact in Imo State, Nigeria. *IMPACT: International Journal of Research in Applied, Natural and Social Sciences (IMPACT: IJRANSS) ISSN (P)*: 2347–4580.

Amangabara G.T., Njoku J.D., Obenade M., 2015. Applying satellite remote sensing and GIS tools in the study of gully erosion. *Journal of Scientific Research and Reports* 4(3): 253–264. DOI 10.9734/jsrr/2015/12753.

Ameri A.A., Pourghasemi H.R., Cerda A., 2018. Erodibility prioritization of sub-watersheds using morphometric parameters analysis and its mapping: A comparison among TOPSIS, VIKOR, SAW, and CF multi-criteria decision-making models. *Science of the Total Environment* 613–614: 1385–1400. DOI 10.1016/j.scitotenv.2017.09.210.

Anejionu O.C.D., Nwilo P.C., Ebinne E.S., 2013. *Long term Assessment and mapping of erosion hotspots in southeastern Nigeria.* A paper presented at FIG Working Week 2013 Environment for Sustainability Abuja, Nigeria, 6th–10th May 2013.

Arshad M.A., Martin S., 2002. Identifying critical limits for soil quality indicators in agro-ecosystems. *Agriculture, Ecosystems & Environment* 88(2): 153–160. DOI 10.1016/s0167-8809(01)00252-3.

Asfaw D., Workineh G., 2019. Quantitative analysis of morphometry on Ribb and Gumara watersheds: Implications for soil and water conservation. *International Soil and Water Conservation Research* 7(2): 150–157. DOI 10.1016/j.iswcr.2019.02.003.

Bernard J., Bingner R., Dabney S., Langendoen E., Lemunyon J., Merkel W., Theurer F., Wells R.R., Widman N., Wilson G., 2010. Ephemeral gully erosion – A national resource concern. *National Sedimentation Laboratory Technical Research Rep,* 69.

Biswas S., Sudhakar S., Desai V.R., 1999. Prioritization of subwatersheds based on morphometric analysis of drainage basin, district Midnapore, West Bengal. *Journal of the Indian Society of Remote Sensing* 27(3): 155–166. DOI 10.1007/bf02991569.

Borrelli P., Robinson D.A., Fleischer L.R., Lugato E., Ballabio C., Alewell C., Meusburger K., Modugno S., Schütt B.,

Ferro V., Bagarello V., Van Oost K., Montanarella L., Panagos P., 2017. An assessment of the global impact of 21st century land use change on soil erosion. *Nature Communications* 8(1): 1–13. DOI 10.1038/s41467-017-02142-7.

Borrelli P., Robinson D.A., Panagos P., Lugato E., Yang J.E., Alewell C., Wuepper D., Montanarella L., Ballabio C., 2020. Land use and climate change impacts on global soil erosion by water (2015–2070). *Proceedings of the National Academy of Sciences* 117(36): 21994–22001. DOI 10.1073/pnas.2001403117.

Capra A., Scicolone B., 2002. SW – Soil and water: Ephemeral gully erosion in a wheat-cultivated area in Sicily (Italy). *Biosystems Engineering* 83: 119–126. DOI 10.1006/bioe.2002.0092.

Carter J.V., Pan J., Rai S.N., Galandiuk S., 2016. ROC-ing along: Evaluation and interpretation of receiver operating characteristic curves. *Surgery* 159(6): 1638–1645. DOI 10.1016/j.surg.2015.12.029.

Channels Television, 2018, September 1. *Gully Erosion Ravages Three Communities in Imo State* [Video file]. Online: youtu.be/l8Dfs8vvfao.

Chiemelu N., Okeke F., Nwosu K., Ibe C., Ndukwu R., Ugwuotu A. 2013. The role of surveying and mapping in erosion management and control: A case of Omagba erosion site, Onitsha, Anambra State, Nigeria. *Journal of Environment and Earth Sciences* 3(11): 11–18.

Chopra R., Dhiman R.D., Sharma P.K., 2005. Morphometric analysis of sub-watersheds in Gurdaspur District, Punjab Using Remote Sensing and GIS Techniques. *Journal of the Indian Society of Remote Sensing* 33: 531–539. DOI 10.1007/bf02990738.

Chuenchum P., Xu M., Tang W., 2020. Predicted trends of soil erosion and sediment yield from future land use and climate change scenarios in the Lancang–Mekong River by using the modified RUSLE model. *International Soil and Water Conservation Research* 8(3): 213–227. DOI 10.1016/j.iswcr.2020.06.006.

Dar R.A., Chandra R., Romshoo S.A., 2013. Morphotectonic and Lithostratigraphic analysis of Intermontane Karewa basin of Kashmir Himalayas, India. *Journal of Mountain Science* 10(1): 1–15. DOI 10.1007/s11629-013-2494-y.

De Araujo J.C., Güntner A., Bronstert A., 2006. Loss of reservoir volume by sediment deposition and its impact on water availability in semiarid Brazil. *Hydrological Sciences Journal* 51(1): 157–170. DOI 10.1623/hysj.51.1.157.

Egboka B.C.E., Okpoko E.I., 1984. Gully erosion in the Agulu-Nanka region of Anambra State, Nigera. Challenges in African Hydrology and Water Resources (Proceedings of the Harare Symposium). IAHS Publ. No. 144.

Ezezika O.C., Adetona O., 2011. Resolving the gully erosion problem in Southeastern Nigeria: Innovation through public awareness and community-based approaches. *Journal of Soil Science and Environmental Management* 2(10): 286–291.

Farhan Y., Anaba O., 2016. Watershed prioritization based on morphometric analysis and soil loss modeling in Wadi Kerak (Southern Jordan) using GIS techniques. *International Journal of Plant and Soil Science* 10: 1–18. DOI 10.9734/ijpss/2016/25321.

Farhan Y., Anbar A., Al-Shaikh N., Mousa R., 2017. Prioritization of semi-arid agricultural watershed using morphometric and principal component analysis, remote sensing, and GIS techniques, the Zerqa River Watershed, Northern Jordan. *Agricultural Sciences* 8(1): 113–148. DOI 10.4236/as.2017.81009.

Farr T.G., Rosen P.A., Caro E., Crippen R., Duren R., Hensley S., Kobrick M., Paller M., Rodriguez E., Roth L., Seal D., Shaffer S., Shimada J., Umland J., Werner M., Oskin M., Burbank D., Alsdorf D., 2007. The shuttle radar topography mission-RG2004. *Reviews of Geophysics* 45(2): 1–33. DOI 10.1029/2005rg000183.

Fayas C.M., Abeysingha N.S., Nirmanee K.G.S., Samaratunga D., Mallawatantri A. 2019. Soil loss estimation using rusle model to prioritize erosion control in KELANI river basin in Sri Lanka. *International Soil and Water Conservation Research* 7(2): 130–137. DOI 10.1016/j.iswcr.2019.01.003.

Forkuor G., Maathuis B., 2012. Comparison of SRTM and AS-TER derived digital elevation models over two regions in Ghana – Implications for Hydrological and Environmental Modeling. *Studies on Environmental and Applied Geomorphology.* DOI 10.5772/28951.

Gajbhiye S., Mishra S.K., Pandey A., 2014. Prioritizing erosion-prone area through morphometric analysis: An RS and GIS perspective. *Applied Water Science* 4(1): 51–61. DOI 10.1007/s13201-013-0129-7.

Gao P., 2013. Rill and gully development processes. In: Shroder, J. (Editor in Chief), Marston, R.A., Stoffel, M. (eds.), *Treatise on geomorphology.* Vol. 7, Mountain and Hillslope Geomorphology, Academic Press, San Diego, CA: 122–131. DOI 10.1016/B978-0-12-374739-6.00156-1.

Harlin J.M., Wijeyawickrema C., 1985. Irrigation and groundwater depletion in Caddo county, Oklahoma. *JAWRA Journal of the American Water Resources Association* 21(1): 15–22. DOI 10.1111/j.1752-1688.1985.tb05346.x.

Hlaing K.T., Haruyama S., Aye M.M., 2008. Using GIS-based distributed soil loss modeling and morphometric analysis to prioritize watershed for soil conservation in Bago river basin of Lower Myanmar. *Frontiers of Earth Science China.* 2(4): 465–478. DOI 10.1007/s11707-008-0048-3.

Horton R.E., 1932. Drainage basin characteristics. *Transactions of the American Geophysical Union* 13: 350–361. DOI 10.1029/tr013i001p00350.

Horton R.E., 1940. An approach toward a physical interpretation of infiltration capacity. *Proc. Soil Sci. Soc. Amer.* 5: 399–417. DOI 10.2136/sssaj1941.036159950005000C0075x.

Horton R.E., 1945. Erosional development of streams and their drainage basins: Hydrophysical approach to quantitative morphology. *Geological Society of America Bulletin* 56: 275–370. DOI 10.1130/0016-7606(1945)56[275:EDOS-AT]2.0.CO;2.

Howard A.D., 1990. Role of hypsometry and planform in basin hydrologic response. *Hydrological Processes* 4(4): 373–385. DOI 10.1002/hyp.3360040407.

Jang T., Vellidis G., Hyman J.B., Brooks E., Kurkalova L.A., Boll J., Cho J., 2013. Model for prioritizing best management practice implementation: Sediment load reduction. *Environmental Management* 51: 209–224. DOI 10.1007/s00267-012-9977-4.

Javed A., Khanday M.Y., Ahmed R., 2009. Prioritization of sub-watersheds based on morphometric and land use analysis using remote sensing and GIS techniques. *Journal of the Indian society of Remote Sensing* 37(2): 261. DOI 10.1007/s12524-009-0016-8.

Jawaharraj N., Kumaraswami K., Ponnaiyan K., 1998. Morphometric analysis of the Upper Noyil basin (Tamil Nadu). *Journal of the Deccan Geographical Society* 36: 1529.

Kabite G., Gessesse B., 2018. Hydro-geomorphological characterization of Dhidhessa River basin, Ethiopia. *International Soil and Water Conservation Research* 6(2): 175–183. DOI 10.1016/j.iswcr.2018.02.003.

Kadam A.K., Jaweed T.H., Kale S.S., Umrikar B.N., Sankhua R.N., 2019. Identification of erosion-prone areas using modified morphometric prioritization method and sediment production rate: A remote sensing and GIS approach. *Geomatics, Natural Hazards and Risk* 10(1): 986–1006. DOI 10.1080/19475705.2018.1555189.

Kumar P., Joshi V., 2016. Characterization of hydro geological behavior of the upper watershed of River Subarnarekha through Morphometric analysis using Remote Sensing and GIS approach. *International Journal of Environmental Sciences* 6(4): 429–447.

Kumaraswami K., Sivagnanam N., 1998. Morphometric characteristics of the vaippar Basin, Tamil Nadu: A qualitative approach. *Indian Journal of landscape System and Ecological Studies* 11(11): 94101.

Lal R., 2003. Soil erosion and the global carbon budget. *Environment international* 29(4): 437–450. DOI 10.1016/S0160-4120(02)00192-7.

Liu X.-l., Tang C., Ni H.-Y., Zhao Y., 2016. Geomorphologic analysis and physico-dynamic characteristics of Zhatai-Gully debris flows in SW China. *Journal of Mountain Science* 13(1): 137–145. DOI 10.1007/s11629-014-3267-y.

Macka Z., 2001. Determination of texture of topography from large scale contour maps. *Geografski Vestnik* 73(2): 53–62.

Maidment D.R., 2002. *ArcHydro GIS for water resources.* Esri Press, California.

Miller V.C., 1953. A quantitative geomorphic study of drainage basin characteristics in the Clinch Mountain area, Virginia and Tennessee, Technical Report 3 NR 389–402, Columbia University, Department of Geology, ONR, New York, NY, USA.

Mohammed A., Adugna T., Takala W., 2018. Morphometric analysis and prioritization of watersheds for soil erosion management in Upper Gibe catchment. *Journal of Degraded and Mining Lands Management* 6(1): 1419–1426. DOI 10.15243/jdmlm.2018.061.1419.

Montanarella L., Pennock D., McKenzie N., Badraoui M., Chude V., Baptista I., Mamo T., Yemefack M., Aulakh M.S., Yagi K., Hong S.Y., Vijarnsorn P., Zhang G.-L., Arrouays D., Black H., Krasilnikov P., Sobocká J., Alegre J., Henriquez C.R., Mendonça-Santos M. de L., Taboada M., Espinosa-Victoria D., AlShankiti A., AlaviPanah S.K., Elsheikh E.A.El M., Hempel J., Arbestain M.C., Nachtergaele F., Vargas R., 2016. World's soils are under threat. *Soil* 2: 79–82. DOI 10.5194/soil-2-79-2016.

Montgomery D.R., Dietrich W.E., 1992. Channel initiation and the problem of landscape scale. *Science* 255: 826–830. DOI 10.1126/science.255.5046.826.

Nag S., Chakraborty S., 2003. Influence of rock types and structures in the development of drainage network in hard rock area. *Journal of the Indian Society of Remote Sensing* 31(1): 25–35. DOI 10.1007/BF03030749.

NASA JPL, 2014. U.S. Releases Enhanced Shuttle Land Elevation Data. NASA Jet Propulsion Laboratory (JPL). http://www.jpl.nasa.gov/news/news.php?release=2014-321 (accessed 21 December 2020).

Nautiyal M.D., 1994. Morphometric analysis of drainage basin, district Dehradun, Uttar Pradesh. *Journal of Indian Society of Remote Sensing.* 22(4): 252–262. DOI 10.1007/BF03026526.

Nelson H.D., Huffman L.H., Fu R., Harris E.L., 2005. Force USPST. Genetic risk assessment and BRCA mutation testing for breast and ovarian cancer susceptibility: Systematic evidence review for the U.S. Preventive Services

Task Force. *Annals of Internal Medicine* 143: 362–79. DOI 10.7326/0003-4819-143-5-200509060-00012.

Nigeria – Erosion and Watershed Management Project, 2012. World Bank Group, Washington, D.C. Online: documents. worldbank.org/curated/en/728741468334143813/Nigeria-Erosion-and-Watershed-Management-Project. documents.worldbank.org/en/publication/documents-reports/documentdetail/728741468334143813/nigeria-erosion-and-watershed-management-project (accessed 13 May 2021).

NIMET [Nigeria Meteorological Agency], 2019. *Seasonal Rainfall Prediction (SRP)*. Periodic Monitoring Report, Saturday, 2 February, 2019. nimet.gov.ng fscluster.org/nigeria/document/nigerian-meteorological-agency-nimet dropbox.com/s/ojqlmvczw8barc6/NIMET%20SRP%20COMPLETE.pdf?dl=0; (accessed 18 December 2019)

Nkonya E., Anderson W., Kato E., Koo J., Mirzabaev A., von Braun J., Meyer S., 2016. *Global cost of land degradation economics of land degradation and improvement – A global assessment for sustainable development*. Springer, Cham: 117–165. DOI 10.1007/978-3-319-19168-3_6.

Nwilo P.C., Olayinka D.N., Uwadiegwu I., Adzandeh A.E., 2011. An assessment and mapping of gully erosion hazards in Abia State: A GIS approach. *Journal of Sustainable Development* 4(5): 196. DOI 10.5539/jsd.v4n5p196.

Obiadi I.I., Nwosu C.M., Ajaegwu N.E., Anakwuba E.K., Onuigbo N.E., Akpunonu E.O., Ezim O.E. 2011. Gully Erosion in Anambra State, South East Nigeria: Issues and solution. *International Journal of Environmental Sciences* 2(2): 795–804.

Ofomata G.E.K., 1965. Factors of soil erosion in the Enugu area of Nigeria. *The Nigerian Geographic Journal* 8(1): 45–59.

Ogbukagu I.K.N., 1976. Soil erosion in the northern parts of the Awka-Orlu Uplands, Nigeria. *Nigerian Journal. Mining & Geology* 13: 6–19.

Okagbue C.O., Uma K.O., 1987. Performance of gully erosion control measures in southeastern Nigeria. Forest Hydrology and Watershed Management (Proceedings of the Vancouver Symposium), Actes du Co11oque de Vancouver, Publ. No. 167.

Okali D., Okpara E., Olawoye J., 2001. The case of Aba and its region, southeastern Nigeria. *International Institute for Environment and Development* 4: 12–20.

Okereke C.N., Onu N.N., 2012. Mapping gully erosion using remote sensing technique: A case study of Okigwe Area, Southeastern Nigeria. *International Journal of Engineering Research and Applications* 2(3): 1955–1967.

Panagos P., Borrelli P., Robinson D., 2019. FAO calls for actions to reduce global soil erosion. *Mitigation and Adaptation Strategies for Global Change*, 25(5): 789–790. DOI 10.1007/s11027-019-09892-3.

Patel A., Katiyar S., Prasad V., 2016. Performances evaluation of different open source DEM using Differential Global Positioning System (DGPS). *The Egyptian Journal of Remote Sensing and Space Science* 19(1): 7–16. DOI 10.1016/j.ejrs.2015.12.004.

Patel D., Gajjar C., Srivastava P., 2013. Prioritization of Malesari mini-watersheds through morphometric analysis: A remote sensing and GIS perspective. *Environmental Earth Sciences*. 69: 2643–2656. DOI 10.1007/s12665-012-2086-0.

Patel D.P., Dholakia M.B., Naresh N., Srivastava P.K., 2012. Water harvesting structure positioning by using geo-visualization concept and prioritization of Mini-Watersheds through morphometric analysis in the lower Tapi Basin. *Journal of the Indian Society of Remote Sensing* 40(2): 299–312. DOI 10.1007/s12524-011-0147-6.

Patton P.C., Baker V.R., 1976. Morphometry and floods in small drainage basins subject to diverse hydrogeomorphic controls. *Water Resources Research* 12(5): 941–952. DOI 10.1029/WR012i005p00941.

Pinheiro E.A.R., Metselaar K., de Jong van Lier Q., de Araújo J.C., 2016. Importance of soil-water to the Caatinga biome, Brazil. *Ecohydrology* 9(7): 1313–1327. DOI 10.1002/eco.1728.

Poesen J., 2018. Soil erosion in the Anthropocene: Research needs. *Earth Surface Processes and Landforms* 43(1): 64–84. DOI 10.1002/esp.4250.

Poesen J., Nachtergaele J., Verstraeten G., Valentin C., 2003. Gully erosion and environmental change: Importance and research needs. *Catena* 50(2–4): 91–133. DOI 10.1016/S0341-8162(02)00143-1.

Pontius R.G., Schneider L.C., 2001. Land-cover change model validation by an ROC method for the Ipswich watershed, Massachusetts, USA. *Agriculture, Ecosystems & Environment* 85(1–3): 239–248. DOI 10.1016/S0167-8809(01)00187-6.

Prasad R., Mondal N., Banerjee P., Nandakumar M., Singh V., 2008. Deciphering potential groundwater zone in hard rock through the application of GIS. *Environmental Geology* 55(3): 467–475. DOI 10.1007/s00254-007-0992-3.

Rahaman S.A., Ajeez S.A., Aruchamy S., Jegankumar R., 2015. Prioritization of sub watershed based on morphometric characteristics using fuzzy analytical hierarchy process and geographical information system – A study of Kallar Watershed, Tamil Nadu. *Aquatic Procedia* 4: 1322–1330. DOI 10.1016/j.aqpro.2015.02.172.

Ratnam K.N., Srivastava Y., Rao V.V., Amminedu E., Murthy K., 2005. Check dam positioning by prioritization of micro-watersheds using SYI model and morphometric analysis — remote sensing and GIS perspective. *Journal of the Indian Society of Remote Sensing* 33(1): 25. DOI 10.1007/BF02989988.

Rawat K.S., Tripathi V.K., Mishra A.K., 2014. Sediment yield index mapping and prioritization of Madia subwatershed, Sagar District of Madhya Pradesh (India). *Arabian Journal of Geosciences* 7(8): 3131–3145. DOI 10.1007/s12517-013-1007-1.

Sartori M., Philippidis G., Ferrari E., Borrelli P., Lugato E., Montanarella L., Panagos P., 2019. A linkage between the biophysical and the economic: Assessing the global market impacts of soil erosion. *Land Use Policy* 86: 299–312. DOI 10.1016/j.landusepol.2019.05.014.

Schumm S.A. 1956. Evolution of drainage systems and slopes in badlands at Perth Amboy, New Jersey. *Bulletin of the Geological Society of America* 67: 597–646. DOI 10.1130/0016-7606(1956)67[597:EODSAS]2.0.CO;2.

Singh V., Singh U., 2011. Basin Morphometry of Maingra River, district Gwalior, Madhya Pradesh, India. *International journal of Geomatics and Geosciences* 1(4): 891–902.

Sreedevi P.D., Srinivasulu S., Kesava Raju K., 2001. Hydrogeomorphological and groundwater prospects of the Pageru River basin by using remote sensing data. *Environmental Geology* 40(8): 1088–1094. DOI 10.1007/s002540100295.

Srivastava V.K., 2003. Role of GIS in natural resources management. In: Thakur B. (ed.), *Perspectives in resource management in developing countries*. Concept Publishing Company, New Delhi: 479–484.

Strahler A.N., 1950. Equilibrium theory of erosional slopes approached by frequency distribution analysis; Part II. *American Journal of Science*, 248(11): 800–814. DOI 10.2475/ajs.248.11.800.

Strahler A.N., 1957. Quantitative analysis of watershed geomorphology. *Transactions of the American Geophysical Union* 38: 913–920. DOI 10.1029/TR038i006p00913.

Strahler A.N., 1964. Quantitative geomorphology of drainage basins and channel networks. In: Chow V.T. (ed.), *Handbook of applied hydrology*. McGraw Hill Book Company, New York: 4–11.

Strahler A.N., 1968. *Quantitative Geomorphology*. In Faibridge, R.W (ed.), *The Encyclopedia of Geomorphology,* Reinhold Book Crop., New York: 898–912. DOI 10.1007/3-540-31060-6_304.

Sun G., Ranson K.J., Kharuk V.I., Kovacs K., 2003. Validation of surface height from shuttle radar topography mission using shuttle laser altimeter. *Remote Sensing of Environment* 88(4): 401–411. DOI 10.1016/j.rse.2003.09.001.

Vaidya N., Kuniyal J.C., Chauhan R., 2013. Morphometric analysis using Geographic Information System (GIS) for sustainable development of hydropower projects in the lower Satluj river catchment in Himachal Pradesh, India. *International journal of Geomatics and Geosciences* 3(3): 464–473.

Valentin C., Poesen J., Li Y., 2005. Gully erosion: Impacts, factors and control. *Catena* 63(2–3): 132–153. DOI 10.1016/j.catena.2005.06.001.

Vanmaercke M., Poesen J., Van Mele B., Demuzere M., Bruynseels A., Golosov V., Bezerra J.F.R., Bolysov S., Dvinskih A., Franki A., Fuseina Y., Guerra A.J.T., Haregeweyn N., Ionita I., Imwangana F.M., Moeyersons J., Moshe I., Samani A.Z., Niacșu L., Rysin I., Ryzhov Yu.V., Yermolaev O.P., Frankl A., 2016. How fast do gully headcuts retreat? *Earth-Science Reviews* 154: 336–355. DOI 10.1016/j.earscirev.2016.01.009.

Verstraeten G., Bazzoffi P., Lajczak A., Rădoane M., Rey F., Poesen J., de Vente J., 2006. Reservoir and pond sedimentation in Europe. *Soil Erosion in Europe* 759–774. DOI 10.1002/0470859202.ch54.

Vollmer D., Pribadi D.O., Remondi F., Rustiadi E., Grêt-Regamey A., 2016. Prioritizing ecosystem services in rapidly urbanizing river basins: A spatial multi-criteria analytic approach. *Sustainable Cities and Society* 20: 237–252. DOI 10.1016/j.scs.2015.10.004.

Wei R., Zeng Q., Davies T., Yuan G., Wang K., Xue X., Yin Q., 2018. Geohazard cascade and mechanism of large debris flows in Tianmo gully, SE Tibetan Plateau and implications to hazard monitoring. *Engineering Geology* 233: 172–182. DOI 10.1016/j.enggeo.2017.12.013.

Yibeltal M., Tsunekawa A., Haregeweyn N., Adgo E., Meshesha D.T., Aklog D., Masunaga T., Tsubo M., Billi P., Vanmaercke M., Ebabu K., Dessie M., Sultan D., Liyew M., 2019. Analysis of long-term gully dynamics in different agro-ecology settings. *Catena* 179: 160–174. DOI 10.1016/j.catena.2019.04.013.

Zhang X., Li X., Feng Y., Liu Z., 2015. The use of ROC and AUC in the validation of objective image fusion evaluation metrics. *Signal Processing* 115: 38–48. DOI 10.1016/j.sigpro.2015.03.007.